Morphology of the groove of the inferior petrosal sinus: application to better understanding variations and surgery of the skull base

Uduak-Obong I. Ekanem[1], Łukasz Olewnik[2], Andrea Porzionato[3], Veronica Macchi[3], Joe Iwanaga[4,5], Marios Loukas[6], Aaron S. Dumont[4], Raffaele De Caro[3], R. Shane Tubbs[4,5,6,7,8,9,10]

[1]Tulane University School of Medicine, New Orleans, LA, USA, [2]Department of Anatomical Dissection and Donation, Medical University of Lodz, Lodz, Poland, [3]Section of Human Anatomy, Department of Neuroscience, University of Padova, Padova, Italy, [4]Department of Neurosurgery, Tulane Center for Clinical Neurosciences, Tulane University School of Medicine, New Orleans, LA, [5]Department of Neurology, Tulane Center for Clinical Neurosciences, Tulane University School of Medicine, New Orleans, LA, USA, [6]Department of Anatomical Sciences, St. George's University, St. George's, Grenada, [7]Department of Structural & Cellular Biology, Tulane University School of Medicine, New Orleans, LA, [8]Department of Surgery, Tulane University School of Medicine, New Orleans, LA, [9]Department of Neurosurgery and Ochsner Neuroscience Institute, Ochsner Health System, New Orleans, LA, USA, [10]University of Queensland, Brisbane, Australia

Abstract: Although adequate venous drainage from the cranium is imperative for maintaining normal intracranial pressure, the bony anatomy surrounding the inferior petrosal sinus and the potential for a compressive canal or tunnel has, to our knowledge, not been previously investigated. One hundred adult human skulls (200 sides) were observed and documented for the presence or absence of an inferior petrosal groove or canal. Measurements were made and a classification developed to help better understand their anatomy and discuss it in future reports. We identified an inferior petrosal sinus groove (IPSG) in the majority of specimens. The IPSG began anteriorly where the apex of the petrous part of the temporal bone articulated with the sphenoid part of the clivus, traveled posteriorly, in a slight medial to lateral course, primarily just medial to the petro-occipital fissure, and ended at the anteromedial aspect of the jugular foramen. When the IPSGs were grouped into five types. In type I specimens, no IPSG was identified (10.0%), in type II specimens, a partial IPSG was identified (6.5%), in type III specimens, a complete IPSG (80.0%) was identified, in type IV specimens, a partial IPS tunnel was identified (2.5%), and in type V specimens, a complete tunnel (1.0%) was identified. An improved knowledge of the bony pathways that the intracranial dural venous sinuses take as they exit the cranium is clinically useful. Radiological interpretation of such bony landmarks might improve patient diagnoses and surgically, such anatomy could decrease patient morbidity during approaches to the posterior cranial fossa.

Key words: Anatomy, Cadaver, Skull base, Dural venous sinus, Bony groove

Corresponding author:
Joe Iwanaga
Department of Neurosurgery, Tulane Center for Clinical Neurosciences, Tulane University School of Medicine, New Orleans, LA 70112, USA
E-mail: iwanagajoeca@gmail.com

Introduction

The inferior petrosal sinus (IPS) is an important paired structure in the posterior drainage system and the shortest route within the skull for draining venous blood from the cavernous sinus (CS) to the junction of the sigmoid sinus and

superior jugular bulb [1-7]. The remnant of the fetal head sinus after it forms the sigmoid sinus, the pre-otic sinus, and proximal ventral myelencephalic vein contributes to the formation of the inferior petrosal sinus [3-8]. The conventional carotid vertebral angiogram/venogram has been an important tool for visualizing the IPS [5], which is important in other ways apart from venous blood drainage. In medical application it is used in bilateral sampling, which is valuable in combination with corticotropin-releasing hormone stimulation both for diagnosing Cushing's disease and also for distinguishing it from ectopic adrenocorticotropic hormone (ACTH) levels [7-12]. Additionally, owing to its position and ease of access, the IPS is routinely used for transvenous embolization of cavernous sinus dural arteriovenous fistulas (CSDAVFs), even in cases when the IPS is radiologically occluded [6, 12-15].

The IPS runs within a bony channel called the inferior petrosal sinus groove (IPSG) [3, 16, 17]. Contributors to the IPSG include the wall of the petro-occipital fissure, the occipital bone, and the petrous portion of the temporal bone [6,18]. The IPS has been extensively studied using microsurgery, magnetic resonance imaging, and variations of computed tomography (CT) as well as angiography [5, 13, 18]. Although major studies have used angiography, Gebarski and Gebarski [18] pioneered an IPS imaging-anatomical correlation that specifically elucidated the morphology of the IPSG, its asymmetrical nature, and its variations. Additionally, a classification system for the IPS has been developed [8].

To our knowledge, while the IPS has been studied in detail, there has been no comparable in-depth study of the IPSG including its overall structure and variations. Doppman et al. [9] demonstrated the importance of the IPS for bilateral sampling. It has been suggested that the contribution of the IPSG to IPS anatomy could be a factor in the rare false-negative results from sampling, but this has yet to be studied. Also, in transvenous embolization of CS fistulas using the IPS, variations in IPS size determined the type of probe and catheter employed [6, 14].

Given the importance of the IPSG, this project serves as the first in-depth study of it. Thorough analysis led to the development of a classification scale to account for differences in the sulci within a skull and among multiple skulls. This classification scale can potentially inform various interventions for pathological states involving the IPS and skull base.
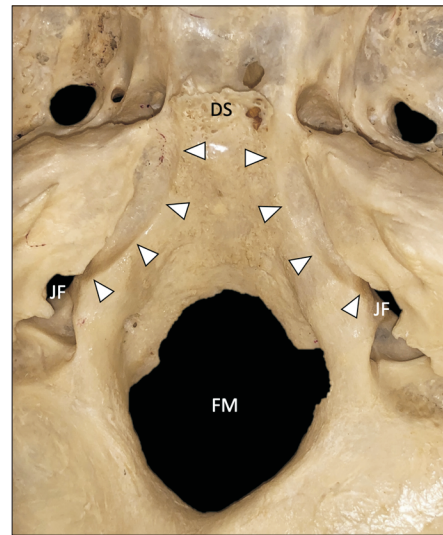

Fig. 1. Superior view of the skull base in a bony specimen. The inferior petrosal sinus grooves (arrowheads) are seen traveling from anteriorly just lateral to the dorsum sellae (DS) to posteriorly into the jugular foramen (JF). FM, foramen magnum.

Materials and Methods

One hundred dry adult human skulls (200 sides) were studied in order to verify the presence of an IPSG at the skull base. The exact age and sex of the specimens were not known. The groove was defined as the bony indentation running from inferolateral to the dorsum sella medially and the apex of the petrous part of the temporal bone laterally, traveling inferiorly along the base of the petrous part of the temporal bone and medial to the jugular tubercle of the occipital bone and terminating at the anteromedial aspect of the jugular foramen. When magnification was necessary, a surgical microscope was used (Zeiss, Oberkochen, Germany). Measurements of these structures were made, and a classification developed to help better describe the anatomy of these structures. Measurements included the maximal width and depth of the IPSG. All measurements were performed using microcalipers (Mitutoyo, Kawasaki, Japan). Statistical analyses were performed (Student's t-test) to discern any differences between sides with significance set at $P<0.05$. Correlation between morphological findings was analyzed using Pearson's correlation coefficient.

Results

We identified an IPSG in the majority of specimens (Fig. 1). The IPSG began anteriorly where the apex of the petrous
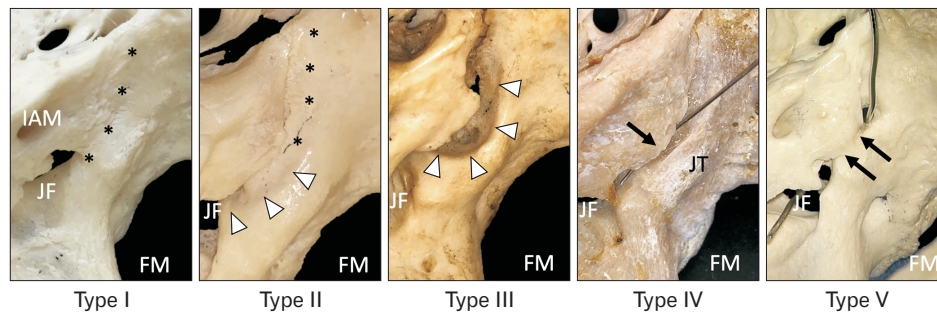
Fig. 2. Five types of inferior petrosal sinus groove (superior view on left sides). Type I: No inferior petrosal sinus groove. Type II: A partial inferior petrosal sinus groove. Type III: A complete inferior petrosal sinus groove. Type IV: A partial inferior petrosal sinus tunnel (the arrow marks the ala of the petrous part of the temporal bone that is contributing to a partial tunnel here with a needle placed within it). Type V: A complete inferior petrosal sinus tunnel (the arrows marks the ala. A metal wire is placed into the complete tunnel created by the ala). IAM, internal acoustic meatus; FM, foramen magnum; JF, jugular foramen; JT, jugular tubercle. The asterisk marks the predicted course of the inferior petrosal sinus but without a bony groove. Arrowheads, inferior petrosal sinus groove.
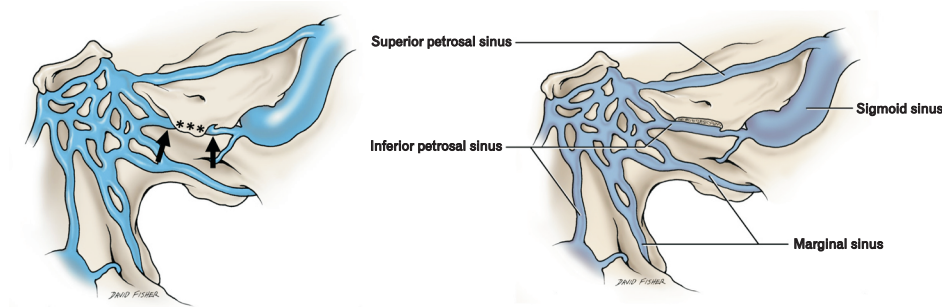

Fig. 3. Schematic drawings of the relationship of the inferior petrosal sinus. On the left, the arrows mark the sinus before and after entering the tunnel of a type V and created by the ala (asterisk). On the right side, the ala is removed to show the inferior petrosal sinus along its entire course.

part of the temporal bone articulated with the sphenoid part of the clivus (crossed in life by Gruber's ligament), traveled posteriorly, in a slight medial to lateral course, primarily just medial to the petro-occipital fissure, and ended at the anteromedial aspect of the jugular foramen. When the IPSGs were grouped into five types (Fig. 2):

Type I: No IPSG (20; 10.0%)

Type II: A partial IPSG (13; 6.5%)

Type III: A complete IPSG (160; 80.0%)

Type IV: A partial IPS tunnel (5; 2.5%)

Type V: A complete tunnel (2; 1.0%)

Partial and complete tunnels (*i.e.*, type IV and type V IPSG) occurred medial to a protuberant part of the petrous part of the temporal bone and lateral to the jugular tubercle of the occipital bone (Fig. 3). This protuberant part of the bone (Fig. 2) was approximately one centimeter wide and extended medially toward the jugular tubercle of the occipital bone and thereby allowed the more lateral part of the IPSG to travel inferior to it when a type IV and converted the IPSG into a tunnel when a type V. One type III IPSG (left side) was related to a jugular foramen that was completely divided by
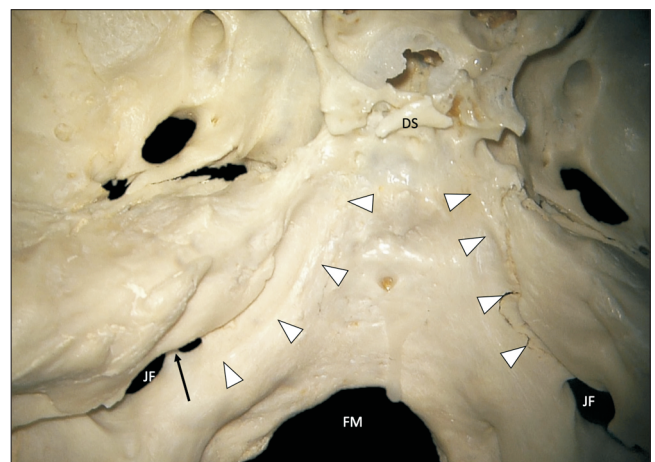

Fig. 4. Skull base sample with an inferior petrosal sinus groove (arrowheads) connecting posteriorly into a bony septated jugular foramen (arrow). DS, dorsum sellae; FM, foramen magnum; JF, jugular foramen.

a bony separation (Fig. 4). Therefore, the IPSG connected to the more anterior part of this split jugular foramen. Complete IPSGs were more common on right sides ($P<0.05$). The
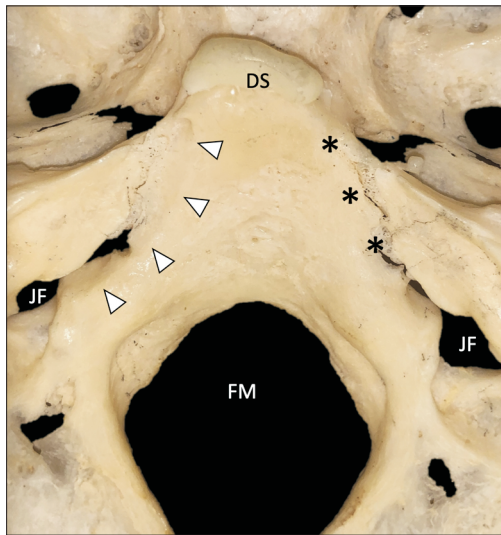
Fig. 5. Skull base sample without an inferior petrosal sinus groove on the right (asterisk, type I) and a groove on the left (arrowheads, type II). DS, dorsum sellae; FM, foramen magnum; JF, jugular foramen.
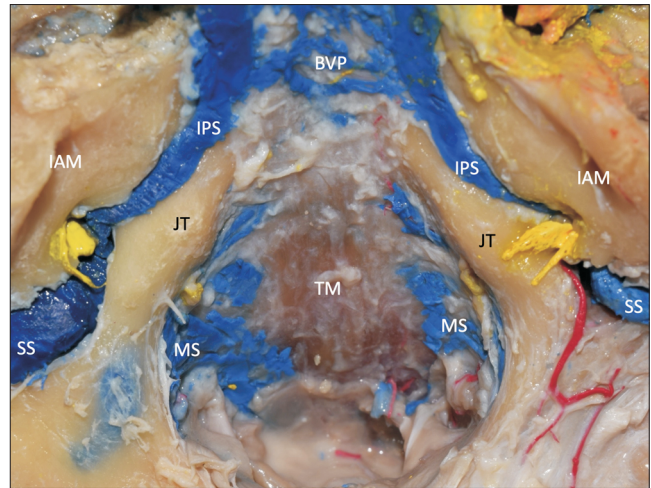

Fig. 6. An example of skull base with blue latex injected into the venous sinuses of the posterior cranial fossa. Note the asymmetry between the left and right inferior petrosal sinuses (IPS). The yellow structures are the stumps of the glossopharyngeal, vagus, and accessory nerves. JT, jugular tubercle; IAM, internal acoustic meatus; TM, tectorial membrane; MS, marginal sinus; BVP, basilar venous plexus; SS, sigmoid sinus.

mean depth of the IPSG was 1.9 mm (0.75–3.2 mm) and the mean width of the grooves was 3.4 (2.1–5.6 mm). The mean length of the IPSG was 25 mm (range 20–28.5 mm). Larger grooves were moderately correlated (r=0.65) to a more prominent jugular tubercle and were more commonly (70%) located on right sides (P<0.05). Larger jugular tubercles were strongly correlated (P=0.70) to the presence of a partial or complete tunnel i.e., types IV and V. An asymmetrical IPSG was common on left and right sides of the same specimen (Figs. 5, 6). No gross pathology of the skull base was identified in any specimen.

Discussion

We identified an IPSG in the majority of specimens. Although some [19] have stated that the IPS overlies the petro-occipital fissure, our findings demonstrated that the IPSG was mostly lateral to this skull base joint. The anatomical-imaging correlation, more specifically axial CT images, by Gebarski and Gebarski [18] revealed a relationship between the size of the IPS and the IPSG (Fig. 6). Their results showed that the deeper the IPSG, the larger the IPS. This conclusion was inferred from results correlating 40 CT studies. Therefore, if a type III IPSG as classified herein is identified on preoperative or preprocedural imaging, a larger IPS should be anticipated. Types IV and V (incomplete and complete tunnels), when present (2.5% and 1.0%, respectively) were
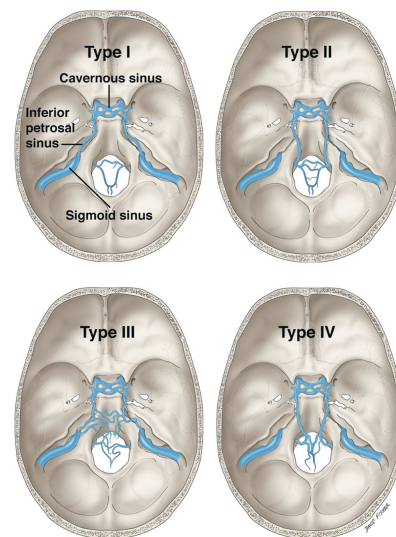

Fig. 7. Shiu et al. [20] classification of the four main variations of the inferior petrosal sinus.

compressive in nature as the dimensions of the pathway for the IPS were less than sides without a tunnel or partial tunnel. Therefore, patients with these types of grooves would be expected to have a small sinus at this location.

Petrosal sinus sampling is a mainstay for diagnosing Cushing syndrome, and for distinguishing this condition from ectopic ACTH levels in the brain with almost 100%

sensitivity [7-12]. Prior to the study by Doppman et al. [9], false-negative rates for this diagnostic method were as low as 5%. A false negative led to delays in transsphenoidal surgery. Sonography revealed a hypoplastic IPS or a plexiform IPS on the microadenoma side compared to the ipsilateral region, contributing to alteration of the venous channels [9]. Our observations of IPSG indicate how its variations in width or depth can lead to an atrophic sinus, implying other possible reasons for false negatives in petrosal sampling for Cushing's disease. Additionally, if these grooves are tunnel in configuration (*e.g.*, types IV and V), microcatheters placed into these patients might meet resistance.

Transvenous embolization for CSDAVFs is reportedly preferred because it gives better outcomes and it is the gold standard for this condition [6, 12-15]. The many other venous routes to the CS include the superior petrosal, facial, and superior ophthalmic veins, but the IPS remains the mainstay for transvenous embolization regardless of whether the condition in the CS is ipsilateral or contralateral, and even when the IPS is occluded [6]. Jia et al. reported some failure in the performance of transvenous embolization through a thrombosed IPS, which necessitated a switch from the micro guidewire to a 0.035-inch guidewire [6]. From our results, an in-depth knowledge of the IPSG and how it affects access to the IPS can help in similar interventions in the future. For example, as with IPS sampling, if these grooves are tunnel in configuration (*e.g.*, types IV and V), guidewires placed into these patients might meet resistance. Furthermore, the IPSG classification scale can serve in modifying the current guidewires to produce newer guidewires with an expanded scale to meet the highlighted variations and to facilitate penetration of the IPS.

As we identified an IPSG in the majority of specimens, as mentioned above, 10% of sides did not have an identifiable IPSG. This is due to either the absence of the IPS or a deviation in its course. Absence of the IPS has been reported at approximately 1% of the population [11]. As an osteological study, we could not verify the course of the IPS but this might imply a variant inferior course or size of the sinus. Shiu et al. [20] have classified IPS variations from the venography of 53 patients, these authors identified four distinct patterns of drainage into the inernal jugular vein (IJV) as follows (Fig. 7):

1. Type I (45% of patients): The most common version where the IPS drains directly in to the IJV

2. Type II (24% of patients): In these cases, the IPS drained into a communicating vein that united the internal jugular bulb with the deep cervical plexus

3. Type III (24% of patients): In type III variants, the IPS exists essentially as a plexus of veins. The cavernous sinus drains into various locations via this plexus

4. Type IV (7% of patients): The IPS, in these cases, is well formed. However, instead of draining into the superior jugular bulb, it drains into the deep cervical plexus of veins

Lastly, we found that an enlarged jugular tubercle correlated to a larger IPSG. Surgically, this relationship would be important as large tubercles are often drilled down for better access to, for example, vertebrobasilar or posterior inferior cerebellar artery aneurysms via a far lateral transcondylar approach [21]. As our study found partial and complete tunnels (*i.e.*, type IV and type V IPSG) medial to a protuberant part of the petrous part of the temporal bone (we suggest terming this the petrous ala) and lateral to the jugular tubercle of the occipital bone, skull base surgeons performing such maneuvers *e.g.*, drilling of the jugular tubercle should be cognizant of the potential for an enlarged IPS in such situations. This relationship could also help predict larger IPS on imaging.

An improved knowledge of the bony pathways that the intracranial dural venous sinuses take as they exit the cranium is clinically useful. Radiological interpretation of such bony landmarks might improve patient diagnoses and surgically, such anatomy could decrease patient morbidity during approaches to the posterior cranial fossa. Based on our study, complete IPSGs were more common on right sides and larger grooves were moderately correlated to a more prominent jugular tubercle and were more commonly located on right sides. Larger jugular tubercles were strongly correlated to the presence of a partial or complete tunnel. To our knowledge, bony tunnels for the IPS have not previously been described.

ORCID

Uduak-Obong I. Ekanem:
https://orcid.org/0000-0001-5538-2649
Łukasz Olewnik: https://orcid.org/0000-0002-6414-9504
Andrea Porzionato:
https://orcid.org/0000-0003-3025-4717
Veronica Macchi: https://orcid.org/0000-0003-2335-6897
Joe Iwanaga: https://orcid.org/0000-0002-8502-7952
Marios Loukas: https://orcid.org/0000-0003-2811-6657
Aaron S. Dumont: https://orcid.org/0000-0002-8077-8992
Raffaele De Caro: https://orcid.org/0000-0002-2307-0277

R. Shane Tubbs: https://orcid.org/0000-0003-1317-1047

Author Contributions

Conceptualization: JI, ASD, RST. Data acquisition: UOIE, ŁO, RST. Data analysis or interpretation: UOIE, JI. Drafting of the manuscript: UOIE, ŁO, AP, VM, JI, ML, ASD, RDC, RST. Critical revision of the manuscript: ŁO, AP, VM, ML, ASD, RDC, RST. Approval of the final version of the manuscript: all authors.

Conflicts of Interest

No potential conflict of interest relevant to this article was reported.

Acknowledgements

References

1. Doepp F, Hoffmann O, Lehmann R, Einhäupl KM, Valdueza JM. The inferior petrosal sinus: assessment by transcranial Doppler ultrasound using the suboccipital approach. J Neuroimaging 1999;9:193-7.

2. Benndorf G, Campi A. Aberrant inferior petrosal sinus: unusual transvenous approach to the cavernous sinus. Neuroradiology 2002;44:158-63.

3. Mortazavi MM, Griessenauer CJ, Krishnamurthy S, Verma K, Loukas M, Tubbs RS. The inferior petrosal sinus: a comprehensive review with emphasis on clinical implications. Childs Nerv Syst 2014;30:831-4.

4. Mitsuhashi Y, Nishio A, Kawahara S, Ichinose T, Yamauchi S, Naruse H, Matsuoka Y, Ohata K, Hara M. Morphologic evaluation of the caudal end of the inferior petrosal sinus using 3D rotational venography. AJNR Am J Neuroradiol 2007;28:1179-84.

5. Paksoy Y, Genç BO, Genç E. Retrograde flow in the left inferior petrosal sinus and blood steal of the cavernous sinus associated with central vein stenosis: MR angiographic findings. AJNR

Am J Neuroradiol 2003;24:1364-8.

6. Jia ZY, Song YS, Sheen JJ, Kim JG, Lee DH, Suh DC. Cannulation of occluded inferior petrosal sinuses for the transvenous embolization of cavernous sinus dural arteriovenous fistulas: usefulness of a frontier-wire probing technique. AJNR Am J Neuroradiol 2018;39:2301-6.

7. Deipolyi AR, Hirsch JA, Oklu R. Bilateral inferior petrosal sinus sampling. J Neurointerv Surg 2012;4:215-8.

8. Tomycz ND, Horowitz MB. Inferior petrosal sinus sampling in the diagnosis of sellar neuropathology. Neurosurg Clin N Am 2009;20:361-7.

9. Doppman JL, Chang R, Oldfield EH, Chrousos G, Stratakis CA, Nieman LK. The hypoplastic inferior petrosal sinus: a potential source of false-negative results in petrosal sampling for Cushing's disease. J Clin Endocrinol Metab 1999;84:533-40.

10. Boolell M, Gilford E, Arnott R, McNeill P, Cummins J, Alford F. An overview of bilateral synchronous inferior petrosal sinus sampling (BSIPSS) in the pre-operative assessment of Cushing's disease. Aust N Z J Med 1990;20:765-70.

11. Miller DL, Doppman JL, Chang R. Anatomy of the junction of the inferior petrosal sinus and the internal jugular vein. AJNR Am J Neuroradiol 1993;14:1075-83.

12. Lv X, Wu Z. Anatomic variations of internal jugular vein, inferior petrosal sinus and its confluence pattern: implications in inferior petrosal sinus catheterization. Interv Neuroradiol 2015;21:769-73.

13. Zhang L, Zeng F, Wang J, Chen F. Finding the inferior petrosal sinus for embolizing cavernous dural arteriovenous fistula using preoperative computed tomography angiography. World Neurosurg 2019;126:e1069-74.

14. Benndorf G, Bender A, Lehmann R, Lanksch W. Transvenous occlusion of dural cavernous sinus fistulas through the thrombosed inferior petrosal sinus: report of four cases and review of the literature. Surg Neurol 2000;54:42-54.

15. Cho YD, Rhim JK, Yoo DH, Kang HS, Kim JE, Cho WS, Han MH. Transvenous microguidewire looping technique for breach of ipsilateral inferior petrosal sinus occlusions en route to cavernous sinus dural arteriovenous fistulas. Interv Neuroradiol 2016;22:590-5.

16. Robert T, Valsecchi D, Sylvestre P, Blanc R, Ciccio G, Smajda S, Redjem H, Piotin M. May the inferior petrosal sinus recanalization during endovascular treatment for carotid-cavernous fistulas increase the risk of sixth nerve palsy? World Neurosurg 2018;116:e246-51.

17. Raghuram K, Durgam A, Sartin S. Assessment of the inferior petrosal sinus on T1-weighted contrast-enhanced magnetic resonance imaging. J Clin Imaging Sci 2018;8:22.

18. Gebarski SS, Gebarski KS. Inferior petrosal sinus: imaging-anatomic correlation. Radiology 1995;194:239-47.

19. Lo WW, Solti-Bohman LG. High-resolution CT of the jugular foramen: anatomy and vascular variants and anomalies. Radiology 1984;150:743-7.

20. Shiu PC, Hanafee WN, Wilson GH, Rand RW. Cavernous sinus venography. Am J Roentgenol Radium Ther Nucl Med

1968;104:57-62.

21. Day JD. Intradural jugular tubercle reduction to enhance exposure via the transcondylar approach: technical note. Neurosurgery 2004;55:247-50; discussion 251.

22. Iwanaga J, Singh V, Ohtsuka A, Hwang Y, Kim HJ, Moryś J, Ravi KS, Ribatti D, Trainor PA, Sañudo JR, Apaydin N, Şengül G, Albertine KH, Walocha JA, Loukas M, Duparc F, Paulsen F, Del Sol M, Adds P, Hegazy A, Tubbs RS. Acknowledging the use of human cadaveric tissues in research papers: recommendations from anatomical journal editors. Clin Anat 2021;34:2-

4.

23. Iwanaga J, Singh V, Takeda S, Ogeng'o J, Kim HJ, Moryś J, Ravi KS, Ribatti D, Trainor PA, Sañudo JR, Apaydin N, Sharma A, Smith HF, Walocha JA, Hegazy AMS, Duparc F, Paulsen F, Del Sol M, Adds P, Louryan S, Fazan VPS, Boddeti RK, Tubbs RS. Standardized statement for the ethical use of human cadaveric tissues in anatomy research papers: recommendations from Anatomical Journal Editors-in-Chief. Clin Anat 2022 Feb 26 [Epub]. https://doi.org/10.1002/ca.23849.